Available online at www.sciencedirect.com

SciVerse ScienceDirect

Ceramics International 39 (2013) 7461–7465

CERAMICS INTERNATIONAL

www.elsevier.com/locate/ceramint

Synthesis and photocatalytic behavior of $BiVO_4$ with decahedral structure

Zhenfeng Zhu*, Lian Zhang, Junqi Li, Juan Du, Yanbin Zhang, Jiaqi Zhou

School of Materials Science and Engineering, Shaanxi University of Science and Technology, Xi'an 710021, PR China

Received 7 November 2012; received in revised form 4 January 2013; accepted 27 February 2013
Available online 7 March 2013

Abstract

Decahedral $BiVO_4$ was successfully synthesized with Tween-80 as a template by the microwave hydrothermal method. The effects of hydrothermal temperature and Tween-80 on crystal phase and morphology of the obtained $BiVO_4$ were investigated. The crystal phase and morphology were characterized by X-ray diffraction, field emission scanning electron microscopy and UV–vis diffuse reflectance spectroscopy. The results indicated that the as-prepared decahedral $BiVO_4$ was monoclinic. The photocatalytic behavior for methylene blue (MB) degradation was enhanced with the assistance of an appropriate amount of hydrogen peroxide (H_2O_2) under visible light irradiation. The photocatalytic tests indicated that the photocatalytic efficiency of decahedral $BiVO_4$ synthesized at 180 °C was 63.5%. However, $BiVO_4$ sample synthesized at 160 °C showed the highest photocatalytic degradation rate, up to 81.6%, due to its small size and crystal defects.

Keywords: Decahedral $BiVO_4$; Photocatalytic; Microwave hydrothermal; MB

1. Introduction

Since different morphologies of inorganic materials were synthesized by controlling the parameters, for instance, crystal form, size, dimensionality, etc., more and more attention has been attracted to the control of morphologies due to the properties being impacted by them. Fabricating complex architectures, especially the highly ordered three-dimensional (3D) superstructures, opens new possibilities to give some insight into the design of functional materials with new properties, such as the flower-like and dendritic $BiVO_4$ mesocrystal [1], the durian-like and octahedral Fe_3O_4 [2] and the nut-like ZnO microcrystal [3].

As an important non-titania based visible-light-driven semiconductor photocatalyst, $BiVO_4$ has become a focus recently because of its unique properties such as ferroelasticity [4], ionic conductivity [5], photocatalytic activities for water splitting [6–9] and degradation of harmful pollutants [10–13]. The investigation results indicate that the photocatalytic behavior of $BiVO_4$ strongly depends on its crystal form [14–17] and morphology [18–20]. Until now, various morphologies of $BiVO_4$ have been synthesized with the assistance of inorganic or organic additives. For instance, Zhou et al. [21] reported that $BiVO_4$ sample with a high photocatalytic behavior was obtained through K_2SO_4 as an inorganic additive, and the control of $BiVO_4$ morphology was achieved in the $Bi(NO_3)_3 \cdot 5H_2O/V_2O_5/K_2SO_4$ hydrothermal system. Moreover, Yang et al. [22] reported that the monoclinic $BiVO_4$ samples of spheres and uniform decahedrons were synthesized in the presence of SDS by tailoring the hydrothermal temperature, and the decahedral $BiVO_4$ had the highest initial photocatalytic reaction rate of O_2 evolution.

Herein, decahedral $BiVO_4$ was synthesized with Tween-80 as the template using the facile microwave hydrothermal method. The effects of hydrothermal temperature and Tween-80 on crystal phase and morphology of the obtained $BiVO_4$ were investigated. Photocatalytic behaviors of $BiVO_4$

*Corresponding author. Tel./fax: +86 29 86168331.
E-mail addresses: nmlab@sust.edu.cn, zhangjesse97@yahoo.com (Z. Zhu).

0272-8842/$ - see front matter
http://dx.doi.org/10.1016/j.ceramint.2013.02.093

samples synthesized at different temperatures were evaluated in the presence of hydrogen peroxide (H_2O_2).

2. Experimental

2.1. Synthesis of decahedral $BiVO_4$

Decahedral $BiVO_4$ was synthesized with the assistance of Tween-80 in microwave hydrothermal conditions. In a typical synthesis, $Bi(NO_3)_3 \cdot 5\,H_2O$ (5 mmol) and NH_4VO_3 (5 mmol) were dissolved in 25 mL of HNO_3 and 10 mL of NaOH with magnetic stirring, separately. Subsequently, these two solutions were mixed together and stirred for 30 min to get a stable mixture. After sedimentation, the supernatant was removed. 30 mL of Tween-80 was added into the above yellow precipitate and stirred for 30 min continuously. Then the mixture was transferred into a 100 mL Teflon-lined autoclave, maintained at 180 °C for 3 h, and naturally cooled down to room temperature. The precipitate was collected by centrifugation, washed with distilled water and ethanol for several times, and then dried in vacuum at 60 °C for 12 h. To investigate the effect of hydrothermal temperature on the crystal phase and morphology, temperatures were changed from 120 °C to 140 °C, 160 °C and 180 °C.

2.2. Characterization

The as-prepared samples were characterized by X-ray powder diffraction (XRD) with a Rigaku D/max 2200 X-ray diffractometer with a high-intensity Cu Kα radiation ($\lambda = 0.15418$ nm). The SEM images were taken on a field emission scanning electron microscope (JSM-6700F, JEOL Japan). Absorption spectrum was measured on a UV–vis spectrophotometer (UV-2550) in the wavelength range of 250–800 nm.

2.3. Photocatalytic test

Photocatalytic behaviors of the $BiVO_4$ samples were evaluated by photocatalytic degradation of methylene blue (MB) dye with the assistance of hydrogen peroxide (H_2O_2) under visible light irradiation. The experiments were performed in a BL-GHX-V multifunctional photochemical reactor (Shanghai Bilon Experiments Equipment Co., Ltd., Shanghai, China) with eight text tubes. And the irradiation was provided by a 500 W Xe lamp. In each experiment, 0.1 g of photocatalyst was added into 30 mL of MB solution (5 mg/L). Before irradiation, the photocatalyst was homogeneously dispersed in MB solution by ultrasonic bath for 20 min, then 0.1 mL of H_2O_2 (30%, w/w) was added into the solution. At once, the solution was magnetically stirred in darkness for 30 min to reach absorption/desorption equilibrium, and exposed to visible light irradiation. The concentration of the MB solution was monitored by measuring its absorbance at 664 nm during the degradation process via a UV–vis spectrophotometer (UV-722s).

3. Results and discussion

3.1. XRD analysis of the $BiVO_4$ samples

The crystal phases of $BiVO_4$ samples were confirmed using the X-ray powder diffraction method. Fig. 1 shows the XRD patterns of the $BiVO_4$ samples synthesized at different hydrothermal temperatures for 3 h. It was found that tetragonal $BiVO_4$ (JCPDS no. 14-0133) formed after the hydrothermal reaction at 120 °C for 3 h. For the sample synthesized at 140 °C (Fig. 1b), the peak of monoclinic $BiVO_4$ was detected along with the peaks of tetragonal $BiVO_4$, which signified that this sample was a mixture of tetragonal and monoclinic $BiVO_4$. As the hydrothermal temperature increased to 160 °C, none of the peaks corresponding to tetragonal $BiVO_4$ were detected and all the diffraction peaks could be indexed to a pure monoclinic $BiVO_4$ which was in conformity to the standard card (JCPDS no. 14-0688, space group: $I2/a$, unit cell parameters: $a = 5.195$ Å, $b = 11.701$ Å, $c = 5.092$ Å). Compared with the tetragonal phase, the monoclinic $BiVO_4$ had a different crystal structure in which the Bi–O polyhedron was more distorted by a $6s^2$ lone pair electron of Bi^{3+} [23]. As shown in Fig. 1c and inset, the peak at 2θ near 19° showed the characteristic split of the monoclinic scheelite phase, demonstrating that a transformation from tetragonal to monoclinic phase had taken place. With the hydrothermal temperature going up to 180 °C, the XRD pattern (Fig. 1d) of the sample was nearly the same as that of the sample (160 °C) except that the intensity was slightly increased. All these results demonstrated that temperature of 160 °C was sufficient for the formation of monoclinic $BiVO_4$ sample.

3.2. SEM images of $BiVO_4$ samples

To investigate the influence of hydrothermal temperature on the morphology of decahedral $BiVO_4$, a series of experiments were carried out by varying the hydrothermal temperatures

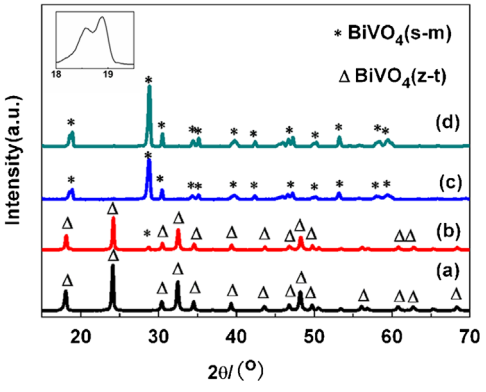

Fig. 1. XRD patterns of the as-prepared samples synthesized at different hydrothermal temperatures for 3 h: (a) 120 °C; (b) 140 °C; (c) 160 °C; and (d) 180 °C. Inset: the widened part of the XRD pattern near 19° showing the characteristic split of the monoclinic scheelite phase.

from 120 °C to 140 °C, 160 °C and 180 °C. Fig. 2 shows the FE-SEM images of the as-prepared samples synthesized at different hydrothermal temperatures for 3 h. When the hydrothermal temperatures were 120 °C and 140 °C, the morphologies of the samples were microspheres with a size of 1–4 μm (Fig. 2a, b). Their corresponding XRD patterns (Fig. 1a, b) confirmed that these microspheres were mainly tetragonal. A further increase to 160 °C, the morphology had a significant change that the premature decahedral structure appeared (Fig. 2c, d). Finally, as the hydrothermal temperature was increased to 180 °C, the sample completely became decahedral structured, as shown in Fig. 2e. Furthermore, the high-magnification FE-SEM image (Fig. 2f) showed that the sample was decahedral. It appeared that the two tops of each octahedron were chopped off in equal amount. Besides, the size of $BiVO_4$ synthesized at 160 °C was smaller than that of $BiVO_4$ synthesized at 180 °C. It was concluded that the hydrothermal temperature played a crucial role in controlling the morphology.

Additionally, Tween-80 played the role of a surfactant in the decahedral forming process. The surface energy was decreased by the surfactant molecules adsorbing on the surface of the $BiVO_4$ nanoparticles. The facets adsorbed with Tween-80 became selective and the growth rate of these facets was reduced [24]. However, this kind of selective adhesion was related to the external conditions, such as the hydrothermal temperature.

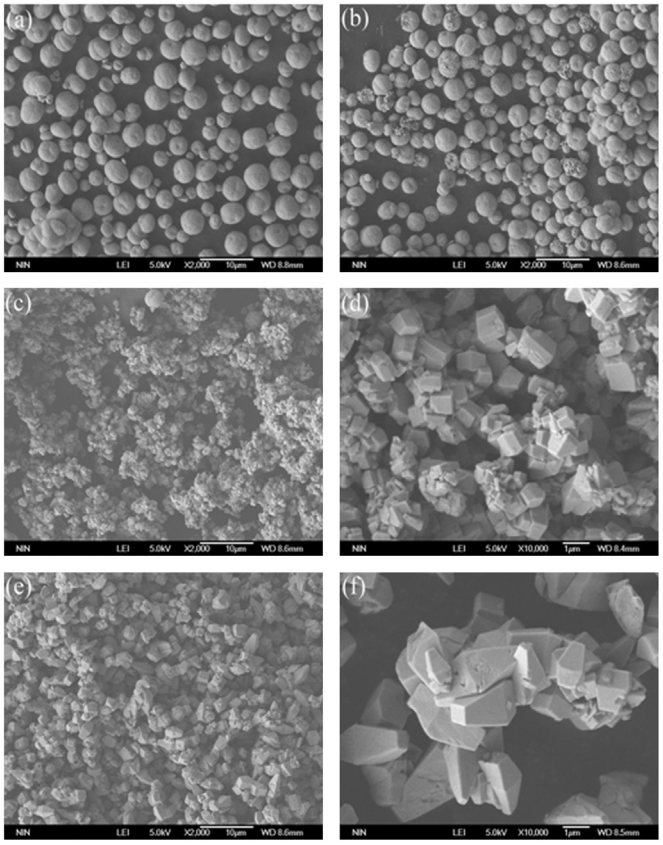

Fig. 2. FE-SEM images of the as-prepared samples synthesized at different hydrothermal temperatures for 3 h: (a) 120 °C; (b) 140 °C; (c, d) 160 °C and (e, f) 180 °C.

3.3. UV–vis diffuse reflectance absorption spectra of $BiVO_4$ samples

The optical properties of the $BiVO_4$ samples were measured using UV–vis spectroscopy. Fig. 3 shows the diffuse reflectance spectra of the $BiVO_4$ samples synthesized at different temperatures. Compared with samples (a) and (b), the absorption edges of samples (c) and (d) extended to nearly 540 nm. Namely, there was a red shift in the band-gap transition. Based on the equation $\alpha h\upsilon = A(h\upsilon - Eg)^{n/2}$ [25], the band gaps of the samples were estimated to be 2.83 eV, 2.80 eV, 2.35 eV, and 2.35 eV, corresponding to the samples of 120 °C, 140 °C, 160 °C, and 180 °C, respectively, as shown in Fig. 3.

Such differences may be ascribed to the changes of crystal phase. The visible-light absorption band with an absorption edge of 450 nm for tetragonal $BiVO_4$ is attributed to the electron transition from O 2p valence band to V 3d conduction band, while the electron transition of monoclinic $BiVO_4$ with an absorption edge of 540 nm is supposed to occur from Bi 6s and O 2p hybrid orbitals to V 3d orbitals. The hybridization of Bi 6s and O 2p levels makes the valence band largely dispersed, which facilitates the mobility of photo-excitated holes, leading to an enhancement of the photocatalytic activity [26].

3.4. Photocatalytic behaviors

The photocatalytic behaviors of the $BiVO_4$ samples synthesized at different temperatures were evaluated by photocatalytic decolorization of MB solution in the presence of H_2O_2 under visible light irradiation. For the samples synthesized at 160 °C and 180 °C, the absorption spectra of MB aqueous solution at different intervals were shown in Fig. 4(A) and (B), respectively. The spectra showed that the intensity of absorption peaks decreased as the degradation time increased, indicating that MB was gradually degradated.

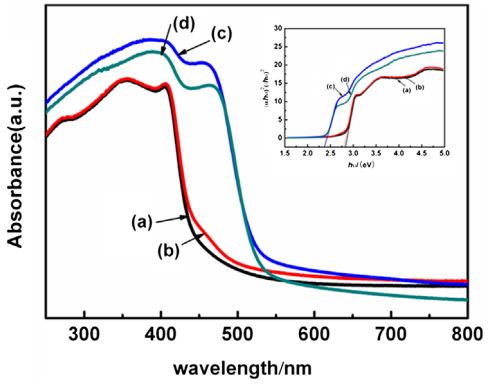

Fig. 3. UV–vis diffuse reflectance spectra of the $BiVO_4$ samples synthesized at different hydrothermal temperatures for 3 h: (a) 120 °C; (b) 140 °C; (c) 160 °C; and (d) 180 °C.

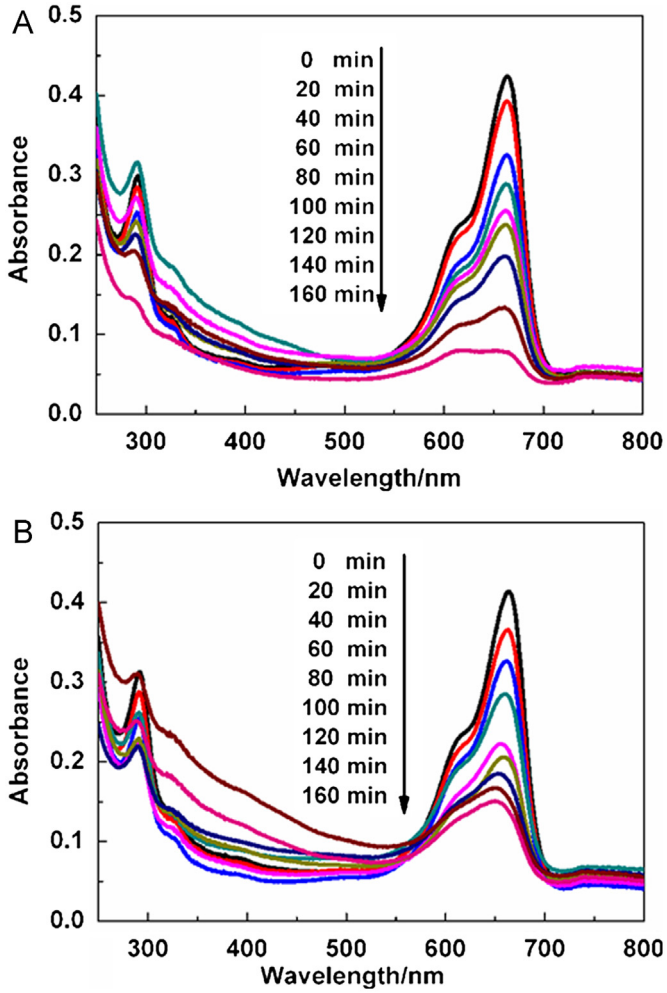

Fig. 4. Absorption spectra of MB aqueous solution at different intervals with the assistance of H_2O_2: (a) $BiVO_4$ synthesized at 160 °C and (b) $BiVO_4$ synthesized at 180 °C.

Furthermore, a blue-shift at $\lambda_{max}=664$ nm after 100 min was observed for the sample synthesized at 180 °C, while this phenomenon could not be found for the sample synthesized at 160 °C. Therefore, degradation of MB might take place in different ways. In Fig. 4(A), the absorption maxima position of MB did not change significantly, indicating that demethylation was not the main reaction. At the same time, the blue color of MB disappeared gradually, demonstrating that the chromophoric structure (>C=N–) of MB was destroyed. However, the blue-shift in Fig. 4(B) was ascribed to the demethylation of the aromatic moiety.

The photocatalytic behavior of $BiVO_4$ sample synthesized at 120 °C was not discussed in this section because of its low photocatalytic activity. Fig. 5 represents degradation of MB in the presence of different photocatalysts under visible light irradiation. It was found that the percentage of MB degradation was low for the pure $BiVO_4$ sample, approximately 47% in 160 min. However, the degradation rate increased significantly after 0.1 mL of H_2O_2 was added. Under visible light irradiation for 160 min, the percentages of MB degradation

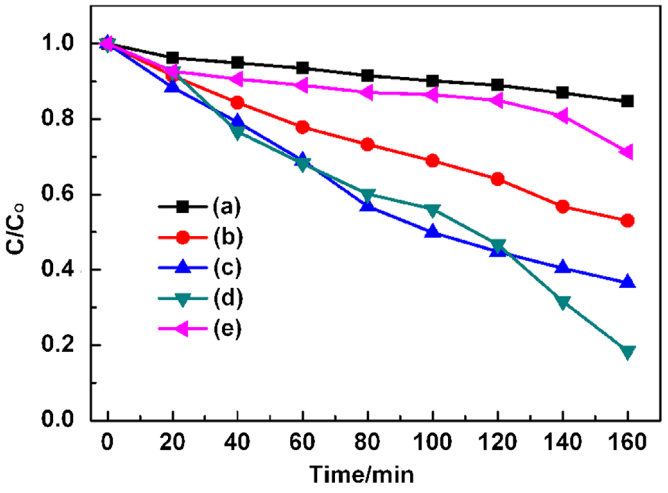

Fig. 5. Degradation of MB in the presence of different photocatalysts under visible light irradiation: (a) only H_2O_2; (b) pure $BiVO_4$ (180 °C); (c) 0.1 mL H_2O_2+$BiVO_4$ (180 °C); (d) 0.1 mL H_2O_2+$BiVO_4$ (160 °C) and (e) 0.1 mL H_2O_2+$BiVO_4$ (140 °C).

were 63.5%, 81.6% and 28.7% at 180 °C, 160 °C and 140 °C, respectively. It should be noted that degradation of MB was observed only with H_2O_2, illustrating that there was a synergic effect between the $BiVO_4$ photocatalyst and H_2O_2.

The possible photocatalytic mechanism in the H_2O_2/$BiVO_4$ system is proposed as follows:

$$BiVO_4 \xrightarrow{h\upsilon} e^- + H^+ \quad (1)$$

The electrons are excited from the valence band to the conduction band by receiving energy from the photons, and the positively charged holes appeared in the valence band (Eq. (1)). The photocatalytic activity is closely related to the efficiency of the photogenerated electron–hole separation [27]. H_2O_2 as an efficient electron scavenger can trap photogenerated electron, and the recombination of electron–hole pairs is restrained (Eq. (2)), so the photocatalytic activity can be improved greatly.

$$H_2O_2 + BiVO_4(e^-) \rightarrow OH^{\bullet} + OH^- \quad (2)$$

The $OH^{\bullet}$ generated from the reaction (Eq. (2)) has strong oxidizing ability and is available to oxidize MB.

In the presence of H_2O_2, $BiVO_4$ samples synthesized at 160 °C and 180 °C exhibited higher photodegradation rate than that of $BiVO_4$ sample synthesized at 140 °C due to their monoclinic crystal phase. It should be noticed that the crystallinity of $BiVO_4$ synthesized at 180 °C was higher than that of $BiVO_4$ synthesized at 160 °C, but the sample (180 °C) showed worse photocatalytic behavior than that of the sample (160 °C). It may be attributed to the imperfect crystal and the small size, resulting in the efficient separation of the electron–hole pairs when the hydrothermal temperature was 160 °C. Moreover, small size allowed efficient transfer of the electron–hole pairs from inside crystal to surface. A large surface area not only supplied more active sites for photocatalytic reaction but also enhanced the separation efficiency of the electron–hole pairs [28].

4. Conclusion

Decahedral $BiVO_4$ was successfully synthesized in the presence of Tween-80 via the microwave hydrothermal method. The $BiVO_4$ microspheres could be derived from a relatively low hydrothermal temperature (e.g., $\leq 140\ ^\circ C$) and the crystal phases were mainly tetragonal phase, while the premature decahedral $BiVO_4$ with pure monoclinic phase could be obtained at 160 °C, and the monoclinic decahedral $BiVO_4$ with a high crystallinity was obtained at 180 °C. In addition, Tween-80 as a morphology-directing reagent was favorable to the formation of decahedral $BiVO_4$. Because of their different crystal phases, the photocatalytic behaviors of $BiVO_4$ samples synthesized at 160 °C and 180 °C were better than that of $BiVO_4$ sample synthesized at 140 °C. The sample synthesized at 160 °C had small size and crystal defects, giving rise to the highest photocatalytic degradation rate, up to 81.6%.

Acknowledgment

This work was financially supported by the China Postdoctoral Science Foundation Founded Project (Nos. 20080440185 and 200902584), the Special Found from Shaanxi Provincial Department of Education (09JK355), and the Postgraduate Innovation Fund of Shaanxi University of Science and Technology.

References

[1] L. Zhou, W.Z. Wang, H.L. Xu, Controllable synthesis of three-dimensional well-defined $BiVO_4$ mesocrystals via a facile additive-free aqueous strategy, Crystal Growth and Design 8 (2008) 728–733.
[2] X.F. Qu, Q.Z. Yao, G.T. Zhou, et al., Formation of hollow magnetite microspheres and their evolution into durian-like architectures, Journal of Physical Chemistry C 114 (2010) 8734–8740.
[3] Y. Zeng, T. Zhang, W.Y. Fu, et al., Fabrication and optical properties of large-scale nutlike ZnO microcrystals via a low-temperature hydrothermal route, Journal of Physical Chemistry C 113 (2009) 8016–8022.
[4] A.R. Lim, K.H. Lee, S.H. Choh, Domain wall of ferroelastic $BiVO_4$ studied by transmission electron microscopy, Solid State Communications 83 (1992) 185–186.
[5] K. Hirota, G. Komatsu, M. Yamashita, et al., Formation, characterization and sintering of alkoxy-derived bismuth vanadate, Materials Research Bulletin 27 (1992) 823–830.
[6] S. Tokunaga, H. Kato, A. Kudo, Selective preparation of monoclinic and tetragonal $BiVO_4$ with scheelite structure and their photocatalytic properties, Chemistry of Materials 13 (2001) 4624–4628.
[7] K. Sayama, A. Nomura, T. Arai, et al., Photoelectrochemical decomposition of water into H_2 and O_2 on porous $BiVO_4$ thin-film electrodes under visible light and significant effect of Ag ion treatment, Journal of Physics and Chemistry B 110 (2006) 11352–11360.
[8] A. Kudo, K. Omori, H. Kato, A novel aqueous process for preparation of crystal form-controlled and highly crystalline $BiVO_4$ powder from layered vanadates at room temperature and its photocatalytic and photophysical properties, Journal of the American Chemical Society 121 (1999) 11459–11467.
[9] J.Z. Su, L.J. Guo, S. Yoriya, et al., Aqueous growth of pyramidal-shaped $BiVO_4$ nanowire arrays and structural characterization: application to photoelectrochemical water splitting, Crystal Growth and Design 10 (2010) 856–861.
[10] L. Zhang, D.R. Chen, X.L. Jiao, Monoclinic structured $BiVO_4$ nanosheets: hydrothermal preparation, formation mechanism, and coloristic and photocatalytic properties, Journal of Physical Chemistry B 110 (2006) 2668–2673.
[11] W.Z. Yin, W.Z. Wang, L. Zhou, et al., CTAB-assisted synthesis of monoclinic $BiVO_4$ photocatalyst and its highly efficient degradation of organic dye under visible-light irradiation, Journal of Hazardous Materials 173 (2010) 194–199.
[12] H.Q. Jiang, H. Endo, H. Natori, et al., Fabrication and photoactivities of spherical-shaped $BiVO_4$ photocatalysts through solution combustion synthesis method, Journal of the European Ceramic Society 28 (2008) 2955–2962.
[13] L. Zhou, W. Wang, S. Liu, et al., A sonochemical route to visible-light-driven high-activity $BiVO_4$ photocatalyst, Journal of Molecular Catalysis A: Chemical 252 (2006) 120–124.
[14] S. Kohtani, M. Koshiko, A. Kudo, et al., Photodegradation of 4-alkylphenols using $BiVO_4$ photocatalyst under irradiation with visible light from a solar simulator, Applied Catalysis B: Environmental 46 (2003) 573–586.
[15] A. Kudo, K. Omori, H. Kato, A novel aqueous process for preparation of crystal form-controlled and highly crystalline $BiVO_4$ powder from layered vanadates at room temperature and its photocatalytic and photophysical properties, Journal of the American Chemical Society 121 (1999) 11459–11467.
[16] X. Zhang, Z.H. Ai, F.L. Jia, et al., Selective synthesis and visible-light photocatalytic activities of $BiVO_4$ with different crystalline phases, Materials Chemistry and Physics 103 (2007) 162–167.
[17] H.B. Li, G.C. Liu, X.C. Duan, Monoclinic $BiVO_4$ with regular morphologies: hydrothermal synthesis, characterization and photocatalytic properties, Materials Chemistry and Physics 115 (2009) 9–13.
[18] L. Zhou, W.Z. Wang, L.S. Zhang, et al., Single-crystalline $BiVO_4$ microtubes with square cross-sections: microstructure, growth mechanism, and photocatalytic property, Journal of Physical Chemistry C 111 (2007) 13659–13664.
[19] W. Liu, L.X. Cao, G. Su, et al., Ultrasound assisted synthesis of monoclinic structured spindle $BiVO_4$ particles with hollow structure and its photocatalytic property, Ultrasonic Sonochemistry 17 (2010) 669–674.
[20] F.X. Wang, M.W. Shao, L. Cheng, et al., The synthesis of monoclinic bismuth vanadate nanoribbons and studies of photoconductive, photoresponse, and photocatalytic properties, Materials Research Bulletin 44 (2009) 1687–1691.
[21] Y. Zhou, K. Vuille, A. Heel, et al., An inorganic hydrothermal route to photocatalytically active bismuth vanadate, Applied Catalysis A: General 375 (2010) 140–148.
[22] T. Yang, D.G. Xia, G. Chen, et al., Influence of the surfactant and temperature on the morphology and physico-chemical properties of hydrothermally synthesized composite oxide $BiVO_4$, Materials Chemistry and Physics 114 (2009) 69–72.
[23] S. Tokunaga, H. Kato, A. Kudo, et al., Selective preparation of monoclinic and tetragonal $BiVO_4$ with scheelite structure and their photocatalytic properties, Chemistry of Materials 13 (2001) 4624–4628.
[24] Y. Khan, S.K. Durrani, M. Siddique, et al., Hydrothermal synthesis of alpha Fe_2O_3 nanoparticles capped by Tween-80, Materials Letters 65 (2011) 2224–2227.
[25] M.A. Butler, Photoelectrolysis and physical properties of the semiconducting electrode WO_2, Journal of Applied Physics 48 (1977) 1914–1920.
[26] J. Tang, Z. Zou, J. Ye, Efficient photocatalytic decomposition of organic contaminants over $CaBi_2O_4$ under visible-light irradiation, Angewandte Chemie International Edition 43 (2004) 4463–4466.
[27] Z.J. Zhang, W.Z. Wang, M. Shang, et al., Photocatalytic degradation of rhodamine B and phenol by solution combustion synthesized $BiVO_4$ photocatalyst, Catalysis Communications 11 (2010) 982–986.
[28] J. Tang, Z. Zou, J. Ye, Effects of substituting Sr^{2+} and Ba^{2+} for Ca^{2+} on the structural properties and photocatalytic behaviors of $CaIn_2O_4$, Chemistry of Materials 16 (2004) 1644–1649.